Reac Kinet Mech Cat (2010) 99:371–379
DOI 10.1007/s11144-009-0133-y

Effects of tungsten on the catalytic activity of Ni–W catalysts for the hydrogenation of aromatic hydrocarbons

Jingyun Sheng · Xiaodong Yi · Feng Li · Weiping Fang

Received: 11 June 2009 / Accepted: 21 July 2009 / Published online: 13 January 2010

Abstract Nano Ni–W catalysts with different tungsten contents prepared by mixing alkaline nickel carbonate with ammonium tungstate show high activity and good sulfur tolerance for hydrogenation of thiophene-containing ethylbenzene. The catalysts were characterized by XRD, TPR, SEM, Raman and BET. The results show that the activity of the catalysts for ethylbenzene hydrogenation is affected profoundly by W loading and the best result was obtained on catalyst with W/Ni ratio equal to 0.16. The increase of activity of the catalyst can be attributed to the interaction between Ni and W doped and the increase of the surface area of the catalyst.

Keywords Ni–W catalyst · Hydrogenation · Aromatic hydrocarbon

Introduction

A high content of aromatic hydrocarbons in diesel fuel will sharply lower the cetane number of diesel oil and contribute significantly to the formation of undesired emissions in the exhaust gas. Under the stringent environmental regulations, the hydrogenation process used to lower the aromatic content in diesel fuel became one of the most important technologies in the petroleum refining industry [1]. In order to produce clean fuel from heavy fractions containing large amounts of aromatic hydrocarbons, both hydrocracking and hydrogenation catalysts with superior catalytic performance are needed. Crude oil typically contains about 1 wt% of sulfur, so the catalysts should be characterized by both high hydrogenation activity and good sulfur tolerance.

J. Sheng · X. Yi (✉) · F. Li · W. Fang (✉)
State Key Laboratory for Physical Chemistry of Solid Surfaces, Engineering Laboratory for Green Chemical Productions of Alcohols, Ethers and Esters, Department of Chemistry, College of Chemistry and Chemical Engineering, Xiamen University, 361005 Xiamen, People's Republic of China
e-mail: xdyi@xmu.edu.cn

W. Fang
e-mail: wpfang@xmu.edu.cn

Two kinds of catalysts are popular for the hydrogenation of aromatic hydrocarbons. One is the metal catalyst, including noble metal catalysts (i.e. Pt, Pd, Ru) [2–7] and non-noble metal catalysts (i.e. Ni, Co) [8–12]. The other type is the sulfide catalyst [13–15]. Metal catalysts possess high activity for the hydrogenation of aromatic hydrocarbons but remain very susceptible to sulfur poisoning. Accordingly, in order to use metal catalysts, the sulfur concentration of the reactant must be decreased to ppm levels or the sulfur tolerance of the catalyst should be greatly improved. On the contrary, the second kind of catalysts has high sulfur tolerance but lower hydrogenation activity. Furthermore, the noble metal catalysts are too expensive for a possible industrial development. It is crucial to develop a catalyst with both high hydrogenation activity and good sulfur resistance.

In this study, tungsten was added to the nano nickel-based catalysts so as to improve the hydrogenation activity and sulfur tolerance of the catalyst. Additionally, the effect of tungsten on the catalytic performances of nickel-based catalysts for ethylbenzene hydrogenation was studied as well.

Experimental

Catalyst preparation

A given quantity of alkaline nickel carbonate was mixed with a solution of ammonium tungstate under agitating to produce a uniform slurry, which was then dried in air at 100 °C for 5 h, followed by calcining at 500 °C for 4 h. All the samples were broken and sieved to 40–60 m before the test. The catalysts are denoted as xWNi, where x is the W/Ni molar ratio.

Catalyst characterization

The surface area (BET) and pore volume of the catalysts were determined with nitrogen as adsorbate at −196 °C on an automatic adsorption instrument (Micromeritics Tristar 3000). The sample was treated at 300 °C for 3 h in vacuum before BET measurement. The XRD characterization was carried out using an X' Pert Pro automatic powder diffractometer operated at 40 kV and 30 mA; Cu K_α ($\lambda = 0.15406$ nm) was used as monochromatized radiation. Raman spectra were recorded with a Renishaw-UV-Vis Raman System 1000 equipped with a CCD detector at room temperature. The 325 nm of the He–Cd laser was used as the exciting source with a power of 30 mW. Scanning electron microscopy (SEM) was carried out by using a field-emission microscope (Leo, 1530) operated at an accelerating voltage of 30 KV. For the temperature programmed reduction experiment (TPR), the sample (50 mg) was pretreated in a flow of O_2/He (20 mL min^{-1}, 20% O_2) at 500 °C for 30 min, cooled to 50 °C, argon was introduced to remove oxygen. Subsequently, the sample was contacted with a flow of Ar/H_2 (20 mL min^{-1}, 5% H_2) while the sample was heated from 50 to 800 °C at a rate of 10 °C min^{-1}. Hydrogen consumption was monitored by an on-line gas chromatograph equipped with a TCD detector after removing the water formed. H_2-TPD measurements were done in a Micromeritics AutoChem II 2920 analyzer. 0.2 g of catalyst sample was filled in a U-shaped quartz reactor tube and a thermocouple was placed onto the top of the sample. All samples were pretreated in H_2 (20 mL min^{-1}) at 500 °C for 1 h. After cooling down to 50 °C, the samples were swept with helium for 60 min and finally the desorption step was performed from 50 to 700 °C at a heating rate of 10 °C min^{-1} and 30 mL min^{-1} of helium total flow.

Catalytic activity measurement

The activity evaluations of the catalysts for ethylbenzene hydrogenation were carried out in a continuous flow high pressure fixed-bed reactor at 1.0 MPa and 200 °C with the catalyst loading of 0.1 mL. The composition of the liquid charge was 300 ppm of thiophene dissolved in ethylbenzene. A liquid flow rate of 1.0 mL h^{-1} and the molar ratio of H_2 to ethylbenzene of 16:1 were used. The catalysts were prereduced for 3 h in a hydrogen flow of 100 mL min^{-1} at 500 °C prior to the activity test. The reaction products were analyzed by using a gas chromatograph equipped with a FID detector.

Results and discussion

Catalyst characterization

BET surface areas of the catalysts are listed in Table 1. It can be seen from Table 1 that the addition of tungsten substantially increases the BET surface area of the catalyst from 29 m^2 g^{-1} for Ni catalyst to 89 m^2 g^{-1} for 0.16WNi catalyst.

Fig. 1 shows the XRD patterns of the Ni-based catalysts that resulted from various contents of tungsten. The XRD patterns of all catalysts show that there are only characteristic peaks of NiO and no characteristic diffraction lines for both WO_3 and mixed Ni–W phases can be observed. The peaks of crystallized NiO are broadened and their intensity decreases gradually with the increase of tungsten content from 0.10WNi to 0.22WNi**,** indicating that the crystalline phase and/or the size of NiO decreases with the increase of W loading.

The Raman spectra of NiO, WO_3 and xWNi catalysts are shown in Fig. 2. In the Raman spectrum of W, three bands at 808, 714 and 274 cm^{-1} can be observed, which are due to the symmetric stretching, asymmetric stretching and bending mode of WO_6 in polycrystalline WO_3 [16]. A broad band around 505 cm^{-1} appears in the Raman spectrum of NiO, which is due to the Ni–O stretching mode of the NiO. In addition to the NiO band at 505 cm^{-1}, the samples 0.10WNi, 0.13WNi, 0.16WNi and 0.19WNi exhibit two bands at 870 and 960 cm^{-1}. The band at 870 cm^{-1} is the characteristic stretching vibration of short terminal O–W–O bonds in the unit cell of WO_4, which suggests the formation of $NiWO_4$ phase and its intensity increases with the increase of W loading [17]. The band at 960 cm^{-1} is attributed to the symmetrical W=O stretching mode of the dispersed tungsten oxide species and its intensity decreases with the increase of W loading [18], indicating that the increase of W in the bimetallic oxide results in more $NiWO_4$ on the oxide surface. For the 0.22WNi sample, the bands ascribed to WO_3 (808, 714 and 276 cm^{-1}) were also observed.

Table 1 Compositions and properties of the catalysts

Catalysts	W/Ni molar ratio	BET surface area (m^2 g^{-1})
Ni	1	29
0.10WNi	0.1:1	65
0.13WNi	0.13:1	77
0.16WNi	0.16:1	89
0.19WNi	0.19:1	80
0.22WNi	0.22:1	72

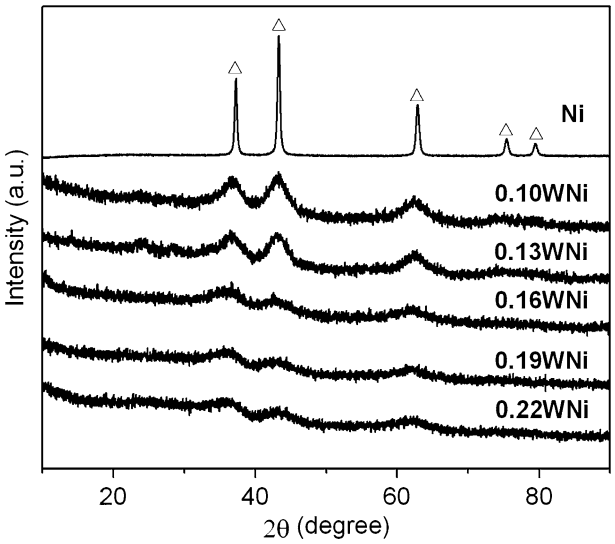

Fig. 1 XRD profiles of the catalysts: NiO (*open triangle*)

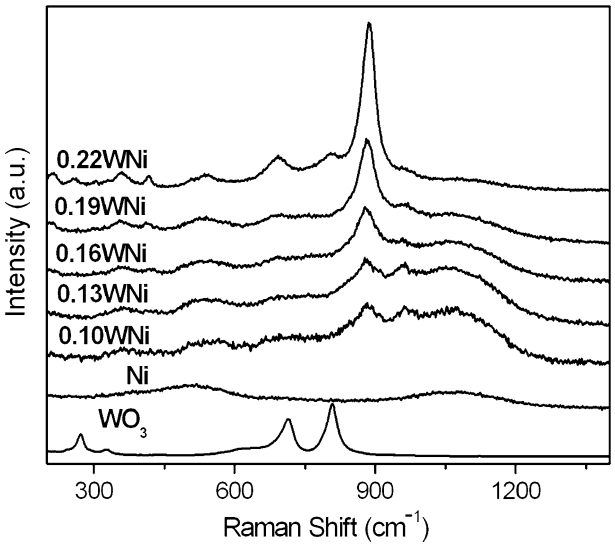

Fig. 2 Raman patterns of the catalysts

Scanning electron micrographs (SEM) of nanosized Ni and 0.16WNi catalysts are shown in Fig. 3. The results of SEM show that only nickel oxide granula of 20–40 nm are visible, but no distinct tungsten aggregates were observed, implying that tungsten is well dispersed within the catalysts. Compared with Ni, the dimension of nanosized 0.16WNi catalyst is smaller and more uniform than that of Ni catalyst.

The TPR profiles of the catalysts are shown in Fig. 4. The TPR pattern of the Ni-based sample shows a peak at 385 °C, which is related to the reduction of crystalline NiO. TPR

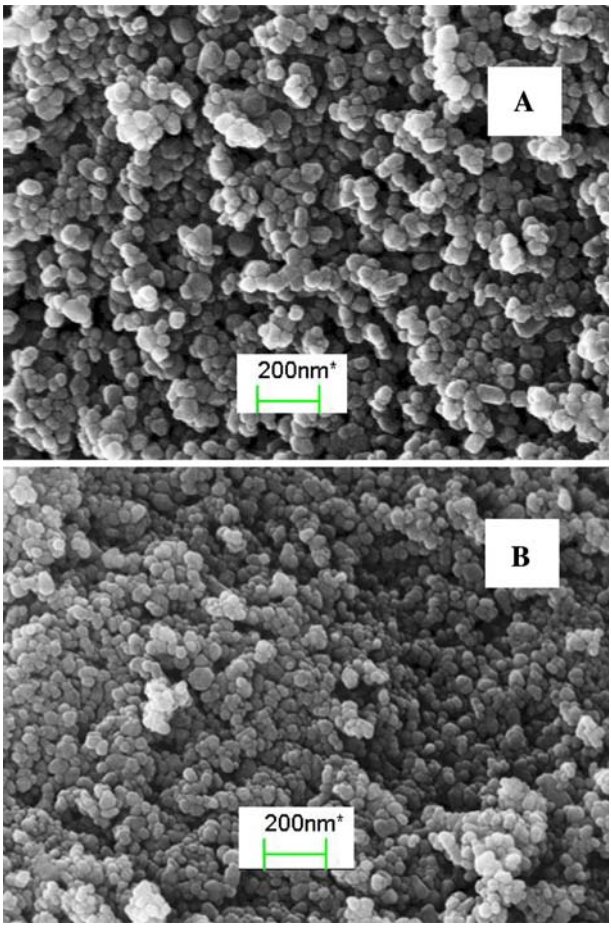

Fig. 3 SEM pictures of the catalysts, **a**: Ni; **b**: 0.16WNi

patterns of the WNi series catalysts consist of two main reduction peaks with maxima near 470 and 600 °C. The reduction peak at 470 °C can be attributed to the reduction of NiO slightly interacting with WO_3. Compared with NiO, the peak shifts to higher value suggesting that the reduction of NiO becomes difficult because of the adding of W. The reduction peak near 600 °C can be attributed to the reduction of $NiWO_4$. In the case of W-doped catalysts, the temperature of maximum H_2-consuming peak shifts to higher value, indicating that an interaction between nickel and tungsten ions takes place and $NiWO_4$ species has formed. This is in agreement with the Raman results.

Fig. 5 shows the H_2-TPD characterization results of the catalysts. There is a desorption peak appears at 130 °C indicating that only one adsorption center of hydrogen exists in the pure nickel catalyst. The TPD patterns of the xWNi catalysts consist of three main desorption peaks centered at 130, 245 and 305 °C. Compared with NiO, the quantity of adsorbed hydrogen of xWNi is higher than that of NiO indicating that the adding of W can help increase the hydrogen adsorption sites of the catalysts. The characterization of TPD shows that a new hydrogen-adsorbed phase formed at high temperature appears and the

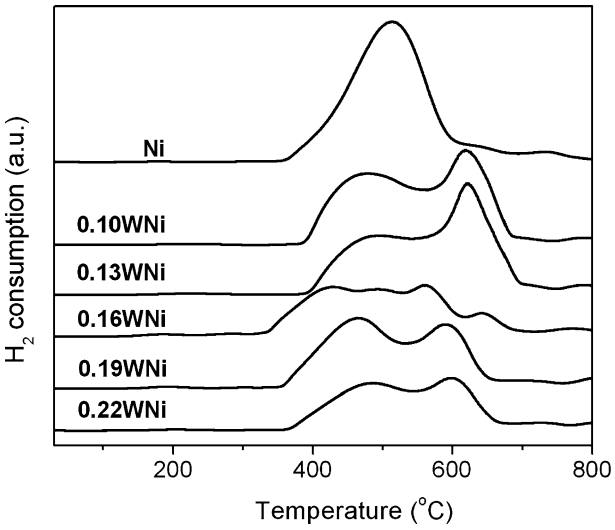

Fig. 4 H_2-TPR profiles of various catalysts

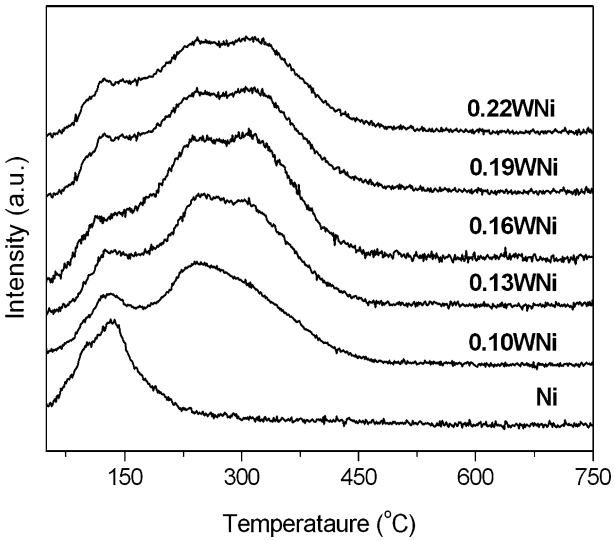

Fig. 5 H_2-TPD profiles of various catalysts

quantity of adsorbed hydrogen increases greatly when W is added to the nickel-based catalysts.

Ethylbenzene hydrogenation

Ethylbenzene hydrogenation is a single hydrogenation reaction when the temperature is below 200 °C, under which ethylcyclohexane was found to be the sole product of the reaction. The results of the hydrogenation of ethylbenzene with 100 and 300 ppm of

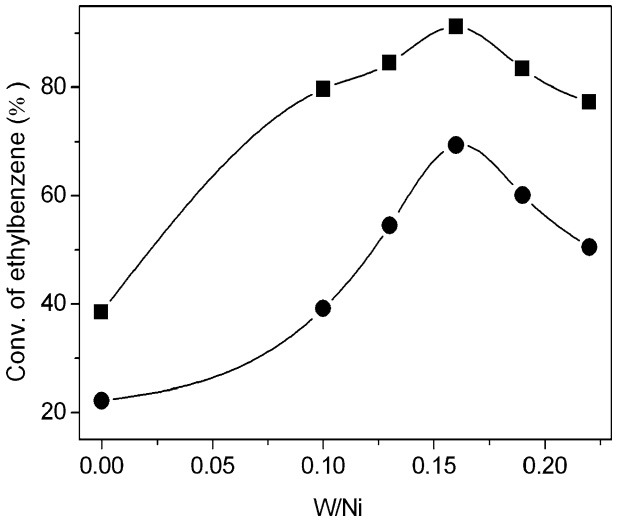

Fig. 6 Conversion of ethylbenzene with 100 ppm (*filled square*) and 300 ppm (*filled circle*) of thiophene over different catalysts. Experiment conditions: LHSV 10.0 h^{-1}, H_2 pressure: 1.0 MPa, reaction temperature: 200 °C, H_2/oil: 16:1

thiophene are shown in Fig. 6. It can be seen that the hydrogenation activity and sulfur tolerance increase with the increase of tungsten proportion and reach a maximum over the catalyst 0.16WNi. But the activity decreases gradually when the W/Ni molar ratio is more than 0.16. The 0.16WNi catalyst exhibits both high activity for hydrogenation of aromatic hydrocarbon and good sulfur tolerance with ethylbenzene conversion of 69.4% under 1.0 MPa, 200 °C and LHSV 10.0 h^{-1}.

Discussion

The above experimental results show that the content of tungsten has a profound effect on the structure and the sulfur tolerance of nano nickel-based catalyst. The Ni-based catalyst with 0.16 of W/Ni ratio shows the highest activity and good sulfur tolerance for the hydrogenation of aromatic hydrocarbons. But the activity decreases gradually when the W/Ni molar ratio is more than 0.16. It is generally accepted that the poisoning mechanism of metal by sulfur compounds involves strong chemisorption of S-containing molecules on the metal sites, followed by its hydrogenolysis, leading to the formation of a stable and inactive Me–S species on the catalyst surface. The higher the electron-donor ability of the metal site is, the stronger the Me–S bond is, and the easier the hydrogenolysis of sulfur compounds is. The S-metal bond is essentially covalent with a slight transfer of electron from the metal to the sulfur atom. Accordingly, an electron-deficient character of Ni sites has been argued by several authors to augment the sulfur resistance of nickel catalysts [19]. The XRD and Raman characterization results show that the Ni–W interaction did occur and $NiWO_4$ species can form on the W-doped samples. Therefore, the Ni–W interaction gives rise to a decrease in the electron density of Ni atoms, and, as a result, weakening the Ni–S bond. Consequently, the equilibrium $Me^0 + H_2S \Leftrightarrow Me\text{–}S + H_2$ shifts toward the left in such a way that the clean surface of Ni metal is highly exposed as active sites for the hydrogenation of thiophene-containing ethylbenzene. This viewpoint is similar to that

proposed by Cooper and Donnis [1] about the improving of sulfur tolerance of noble metal catalyst over acidic carrier and it is also consistent with the H_2-TPR results which show that the W-doped nickel-based catalysts are more difficult to reduce.

In addition to the electronic effect described above, a geometrical effect has to be considered. The characterization results of both BET and SEM show that the addition of tungsten to nickel-based catalyst substantially increases the BET surface areas and that the dimension of nanosized W-doped catalyst is smaller and more uniform than that of the undoped sample. The XRD characterization results also show that tungsten is highly dispersed over the catalyst as an amorphous or microcrystalline phase. It is reasonable to conclude that a significant change on the nickel atom ensembles has occurred on W-doped catalysts. It has been reported that sulfur molecules, such as thiophene and H_2S, undergo multi-site adsorption on nickel surface [20]. It is possible therefore that tungsten plays a diluent role, hindering the NiO ensembles required for the multianchoring and subsequent hydrogenolysis of the sulfur molecules, and then improving the sulfur tolerance. Similar geometrical hypotheses were also suggested to explain the effect of other ionic species on the catalytic properties of metals [20, 21]. When the proportion of tungsten exceeds a certain value, some of the surface active centers will be covered by tungsten particles, so the activity of the catalyst also decreases.

On the other hand, another possible explanation of the effect of tungsten must be taken into account. The tungsten may act as a sulfur acceptor, forming WS_2 and/or NiWS phases during the hydrogenation of thiophene-containing ethylbenzene.

Conclusion

The experimental results show that the addition of tungsten has a profound effect on the structure and the sulfur tolerance of nano nickel-based catalyst. Physico-chemical characterization indicates that the interaction between Ni and W doped did occur $NiWO_4$ species were formed on the W-doped samples, which is responsible for forming a new hydrogen-adsorbed phase at high temperature and increasing adsorbed hydrogen greatly on the catalysts. The results show that the Ni-based catalyst with 0.16 of W/Ni ratio possesses the highest activity and good sulfur tolerance for the hydrogenation of aromatic hydrocarbons. The increase of activity of the catalyst can be attributed to the formation of $NiWO_4$ phase, the uniform distribution of nano-NiO particles on the surface of the catalyst and the increase of the surface area of the catalyst. On the other hand, the presence of tungsten also covers a part of nickel surface, hindering the adsorption of sulfur compounds. Thus, the tungsten-containing Ni-based catalysts are more sulfur resistant.

Acknowledgments This work was supported by the National Basic Research Program of Republic of China under grant 2004CB217805 and 2010CB226903.

References

1. Cooper BH, Donnis BBL (1996) Aromatic saturation of distillates: an overview. Appl Catal A: Gen 137:203
2. Barone G, Duca D (2002) Ab initio study of structure and energetics of species involved in the 2, 4-dinitro-toluene hydrogenation on Pd catalysts. J Mol Struct: Theochem 584:211
3. L'Argentiere PC, Cagnola EA, Liprandi DA, Martnez MCR, Lecea CSM (1998) Aromatic saturation of distillates: an overview. Appl Catal A: Gen 172:41

4. Poondi D, Vannice MA (1996) Competitive hydrogenation of benzene and toluene on palladium and platinum catalysts. J Catal 161:742
5. Sugioka M, Sado F, Kurosaka T, Wang X (1998) Hydrodesulfurization over noble metals supported on ZSM-5 zeolites. Catal Today 45:327
6. Koo-amornpattana W, Winterbottom JM (2001) Pt and Pt-alloy catalysts and their properties for the liquid-phase hydrogenation of cinnamaldehyde. Catal Today 66:277
7. Alexeev OS, Graham GW, Shelef M, Gates BC (2000) γ-Al_2O_3-supported Pt catalysts with extremely high dispersions resulting from Pt–W interactions. J Catal 190:157
8. Rynkowski J, Rajski D, Szyszka I, Grzechowiak JR (2004) Effect of platinum on the hydrogenation activity of nickel catalysts. Catal Today 90:159
9. Tjandra S, Zaera F (1996) A surface science study of the hydrogenation and dehydrogenation steps in the interconversion of C_6 cyclic hydrocarbons on Ni(100). J Catal 164:82
10. Boudjahem AG, Monteverdi S, Mercy M, Bettahar MM (2003) Acetylene cyclotrimerization over Ni/SiO_2 catalysts in hydrogen atmosphere. Appl Catal A: Gen 250:49
11. Turaga UT, Song CS (2003) MCM-41-supported Co–Mo catalysts for deep hydrodesulfurization of light cycle oil. Catal Today 86:129
12. Backman LB, Rautiainen A, Krause AOI, Lindblad M (1998) A novel Co/SiO_2 catalyst for hydrogenation. Catal Today 43:11
13. Marchal N, Mignard S, Kasztelan S (1996) Aromatics saturation by sulfided nickel–molybdenum hydrotreating catalysts. Catal Today 29:203
14. Breysse M, Cattenot M, Kougionas V, Lavalley JC, Mauge F, Portefaix JL, Zotin JL (1997) Hydrogenation properties of ruthenium sulfide clusters in acidic zeolites. J Catal 168:143
15. Elazarifi N, Chaoui MA, Ouassouli AE, Ezzamarty A, Travert A, Leglise J, Menorval LC, Moreau C (2004) Hydroprocessing of dibenzothiophene, 1-methylnaphthalene and quinoline over sulfided NiMo-hydroxyapatite-supported catalysts. Catal Today 98:161
16. Chan SS, Wachs IE, Murrell LL (1984) Relative Raman cross-sections of tungsten oxides: [WO_3, $Al_2(WO_4)_3$ and WO_3/Al_2O_3]. J Catal 90:150
17. Xiao TC, Wang HT, York APE, Williams VC, Green MLH (2002) Preparation of nickel–tungsten bimetallic carbide catalysts. J Catal 209:318
18. Vuurman MA, Wachs IE, Hirt AM (1991) Structural determination of supported vanadium pentoxide–tungsten trioxide–titania catalysts by in situ Raman spectroscopy and x-ray photoelectron spectroscopy. J Phys Chem 95:9928
19. Guerin M, Breysse M, Frety R, Tifouti K, Marecot P, Barbier J (1987) Resistance to sulfur poisoning of metal catalysts: dehydrogenation of cyclohexane on Pt/Al_2O_3 catalysts. J Catal 105:144
20. Diaz A, Odrizola JA, Montes M (1998) Influence of alkali additives on activity and toxicity of H_2S and thiophene over a Ni/SiO_2 catalyst. Appl Catal A: Gen 166:163
21. Figoli NS, Largentiere PC, Arcoya A, Seoane XL (1995) Modification of the properties and sulfur resistance of a Pd/SiO_2 catalyst by La addition. J Catal 155:95